ARTICLES

Conformational Effects on Excitation Transport along Conjugated Polymer Chains

Bernard Van Averbeke and David Beljonne*

Laboratory for Chemistry of Novel Materials, University of Mons-Hainaut, Place du Parc 20, 7000 Mons, Belgium

Received: December 9, 2008

The dynamics of energy transport along rigid rod conjugated polymer—poly(*p*-phenylenebutadyine)—chains is modeled with a special emphasis on the role of conformational disorder. A simple random growth algorithm based on torsion potentials with increasing stiffness yields polymer chains with increasing degree of conjugation and narrower energetic distributions. Despite the fact that the average hopping rate between two subunits is reduced (because the decrease in electronic coupling overwhelms the increase in spectral overlap), a more efficient excitation motion along chains with longer conjugated segments is predicted, in good agreement with recent experiments. This points to the central role of conformational disorder on intrachain energy diffusion in conjugated polymers.

I. Introduction

The need for fast and sensitive optical response in (bio)-chemical sensing applications (medical diagnostics, pollution control, detection of ionic or molecular species, etc.) has driven a lot of research activities toward the design of new photoactive molecular materials.[1] In particular, luminescent conjugated polymers have shown promising features as light harvesting and sensitizing systems.[2−15] The amplified sensory response that has been reported in conjugated polymers in comparison to analogous molecules is usually ascribed to collective effects among the monomer units along polymer chains. However, the mechanism ruling this synergetic effect is still unclear; more specifically, the relative importance of through-space (TS) versus through-bond (TB) interactions is still open to debate.[16−18] In the limiting case of strong electronic couplings between the repeating units along the chain, the latter behave as a single quantum object with fully delocalized excited states. On the other hand, for weak interactions, the electronic excitations tend to self-localize because of coupling to intramolecular vibrations and diffuse incoherently through a sequence of hopping events. This spatial confinement of electronic excitations in conjugated polymers is also induced by the presence of both energetic and conformational disorder. A number of experimental[19,20] and theoretical[21,22] investigations support a multichromophoric picture for conjugated polymers. Upon light absorption, the photoinduced electronic excitations funnel through the energy landscape arising from the distribution of conjugation lengths and site energies to reach low-energy chromophores where light emission takes place. Note that the emissive species could correspond to extended conjugated segments in floppy polymers characterized by a broad distribution of conformational subunits, aggregates formed by intermolecular interactions in rigid-rod structures or resulting from coiling of flexible polymers, as well as chemical or structural impurities.

Recent spectroscopic investigations have shown that the efficiency of energy diffusion along poly(*p*-phenyleneethynylene)s (PPE) chains is significantly improved when the polymer is dissolved in a nematic liquid crystalline (LC) phase rather than in a conventional organic solvent.[23] It was argued that the increase in conjugation in the straightened and planarized polymer chains in the LC environment promotes large TB electronic couplings that result in a continuous π-pathway mediating energy transport. On the modeling side, TB effects can be accounted for by supplementing localized excitations with charge-transfer configurations, as described by Scholes et al.[24] and Thompson et al.[25] Because they reflect conjugation, TB couplings are deemed down in presence of large twist angles between the monomers. Modeling studies performed at the semiempirical level suggest that long conjugated segments separated by conformational kinks interact mostly through space, especially after geometric relaxation in the excited state.[18] Thus, a hopping model appears as a reasonable starting point to depict energy transport along polymer chains, where the influence of increased conjugation can be accounted for through the choice of the chromophoric size distribution. Namely, rigid-rod polymer chains with higher intramolecular order are expected to yield an increased average conjugation length and a reduced distribution width compared to floppy chains. Ideally, this distribution should be time-dependent in case the chromophores evolve with timescales that are commensurate with excitation diffusion times.

Here, we address the role of conformational fluctuations on the nature and dynamics of energy carriers in phenylenebutadyine-based conjugated polymers. The influence of an environment favoring more planar structures, such as the LC phase discussed previously, is taken into account by tweaking the shape of the torsion potential well used to generate random polymer chains. We distinguish between static and dynamic conformational defects. Static kinks involve large torsion angles between conformational subunits that evolve slowly in time and are assumed to act as conjugation breaks over timescales that are long compared to excitation motion. These subunits, however,

* To whom correspondence should be addressed. E-mail: David@averell.umh.ac.be.

10.1021/jp810815d CCC: $40.75
Published on Web 03/04/2009

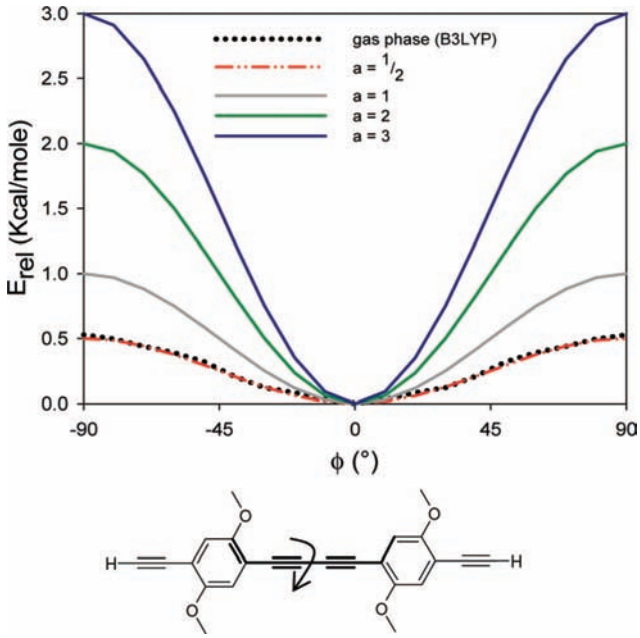

Figure 1. Torsion potentials used in the random chain-growth algorithm and representation of the dihedral angle between two successive units.

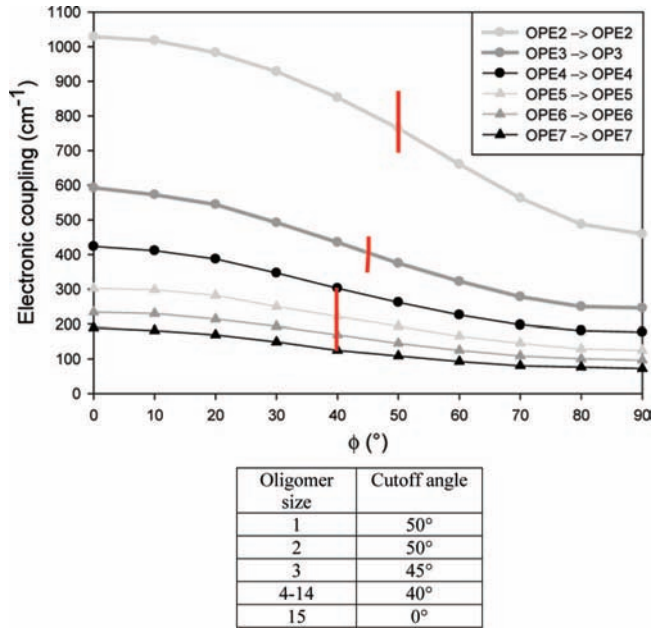

Oligomer size	Cutoff angle
1	50°
2	50°
3	45°
4-14	40°
15	0°

Figure 2. Electronic coupling as a function of dihedral angle ϕ for several oligomer lengths and corresponding values of cutoff for conjugation. The vertical bars in the chart depict the inflection point.

can undergo rapid bond-length reorganization processes mediated by fast (subpicoseconds), high-frequency, stretching/breathing modes as well as local planarization of the conjugated segments associated with libration modes spanning a broad range of timescales (1−100 ps).[26−28] In our simulations, we treat the high-frequency modes as instantaneous (in comparison to energy hopping events), whereas two opposite, extreme, scenarios are considered for the soft torsion modes: complete conformational relaxation and thermalization before hopping or hot energy transfer from the unrelaxed, twisted, ground-state conformation.

II. Modeling Excitation Motion along Multichromophoric Polymer Chains

Polymer chains were generated from a random growth algorithm based on the potential energy surface (PES) for rotation around the single bonds between two subsequent phenylenebutadyine units (torsion angle ϕ). This potential has been calculated at the density functional theory level,[29,30] by using the B3LYP functional[31,32] and the 6-31G(d) basis set.[33] In agreement with previous works on related systems,[34,35] the torsion PES in the gas phase is very flat around the fully planar equilibrium geometry, with a barrier height between the planar and perpendicular conformations of 0.53 kcal/mol, see Figure 1. Thus, thermal energy will likely yield a broad distribution of conformers differing by the amount of interunit twisting at room temperature. Note that the potential energy curve around the equilibrium conformation can be very well fitted by the function $a \sin^2(\phi)$ with $a = 1/2$; see Figure 1.

As discussed above, embedding the phenylene-based polymer chains into a LC environment is expected to result in a stiffer torsion potential, as emphasized by the red-shifted and more structured photoluminescence spectrum compared to solution.[23] To mimic this effect, we have adopted a very simple scheme where the prefactor a in the equation above is varied between the gas phase value 0.5 up to 3, thereby also increasing the barrier height in the same proportion; see Figure 1. For each potential, a total of 100 chains with a physical length of 100 repeating units was built by randomly picking the torsion angles ϕ into the corresponding Boltzmann populations at 300 K.

According to previous investigations, the TB contribution to the electronic coupling decreases with the torsion angle, ϕ, between the monomer units of a polymer because of the diminishing overlap between the π orbitals, whereas the TS interactions are insensitive to ϕ.[18] Both TB and TS couplings are reduced when the size of the interacting chromophores increases as a result of wave-function dilution effects. For sufficiently large torsion angles between two successive units, the electronic conjugation is broken, which yields weakly coupled chromophoric units. Because of the dependence of TB and TS interactions with size, the cutoff value above which the chain can be delineated into two conjugated subsegments depends on the length of the segments. Along the same line as that described in ref 18, we have calculated the overall (TB + TS) electronic coupling for symmetric pairs of chromophores separated by a torsion defect, as a function of the chromophore size.

Figure 2 shows a decrease of the coupling (mostly due to the TB contribution) with ϕ along a sigmoid-like evolution; we have chosen to use the inflection point in the curve as the threshold value for conjugation disruption (we have checked that this choice does not affect the overall picture described below). As expected, the cutoff angle reduces from 50° for dimers down to 40° for hexamers. With this information in mind, monomer units are added one by one, and a static conjugation break is registered once a repeating unit is linked to the growing oligomer with a torsion angle exceeding the threshold value for that oligomer. Note that to avoid the formation of chromophores that could not be handled by the theoretical approach used to compute the hopping rates, the maximum size of the chromophores has been set to 15 repeating units—the length-dependent photophysical properties of the chains, namely, the electronic excitation energy, are fully converged by then.

Within the framework of the weak coupling limit of radiationless transition theory, resonant energy transfer can be described accurately by using an improved Förster model, wherein the electronic matrix elements are calculated from a multicentric atomic representation of the transition moments,

that is, atomic transition densities,[36−41]

$$V_{da} = \frac{1}{4\pi\varepsilon_0}\sum_m \sum_n q_d(m)\, q_a(n)\, V(m,n) \qquad (1)$$

where the sum involves all atomic sites m (n) on the donor d (acceptor a) and $V(m,n)$ is the electron−electron interaction potential (here taken to be the Mataga−Nishimoto potential as implemented in ZINDO).[42] The transition densities have been computed at the INDO/SCI[43] level while accounting for an increased number of molecular orbitals with chromophore size in the active space (in order to obtain size-consistent excitation energies and transition dipole moments). Note that all electronic couplings have been calculated on the ground-state geometric configurations of the chromophores, thus neglecting the possible reshuffling of the transition densities upon geometric relaxation.

For weakly coupled molecules, the hopping rate from donor d to acceptor a, k_{da}, is given by the Fermi Golden rule:

$$k_{da} = \frac{2\pi}{\hbar}|V_{da}|^2 J_{da} \qquad (2)$$

In eq 2, J_{da} represents the spectral overlap between the donor emission and acceptor absorption spectra normalized on an energy scale. The optical spectra are simulated by using an undistorted, displaced, harmonic oscillator model and accounting for two effective vibrational modes: (i) a high-frequency mode (at 1450 cm^{-1}) representative of the dominant carbon−carbon stretching and ring breathing vibrational motions in phenylenebutadyine-based conjugated polymers and (ii) a low-frequency libration mode (at 80 cm^{-1}). The frequency associated to the effective stretching mode considered here has been derived from the mean energy spacing between the main vibronic bands of the experimental spectra of PPE in LC phases, whereas the frequency associated to the ring-torsional mode is the theoretical value obtained by Karaburnaliev and Bittner for oligo(*p*-phenylene)s.[44] Coupling of the electronic excitations to the soft mode will drive the conjugated chains into more planar conformations. The Huang−Rhys factors, S_i, associated to each vibrational mode with frequency ν_i are extracted from the corresponding relaxation energies E_i^{rel} by using

$$S_i = \frac{E_i^{rel}}{h\nu_i} \qquad (3)$$

The Huang−Rhys factor, S_i, is a direct measure of the change in equilibrium geometry along normal mode i when going from the ground state to the lowest electronic excited state. To disentangle the contributions from the two effective modes retained in our model, we have performed INDO/SCI excited-state calculations on chromophores that adopt (i) a fully planar configuration and the AM1[45] ground-state geometrical parameters (i.e., bond lengths and angles) and (ii) a planar conformation and the relaxed excited-state geometry (as optimized at the AM1/SCI level.[46,47] The energy difference between the INDO/SCI vertical excitation energies computed for the chromophores generated from the random growth algorithm and the planar conformers with the same number of repeating units is then the relaxation energy associated to the (effective) soft libration mode. Likewise, we calculate the energy gain induced by coupling to the high-frequency mode from the difference between the INDO/SCI vertical transition energies obtained for the (planar) AM1 ground-state and AM1/SCI excited-state geometries.

As described in the introduction section, we distinguish static from dynamic conformational defects in our simulations. Static defects disrupt the conjugation and result in chromophores the lifetimes of which are long compared to excitation hopping and decay. These are identified from the size-dependent threshold values for torsion angles according to the scheme described previously. As for the dynamic defects, two limiting cases have been considered: either hopping takes place from the chromophores in their twisted conformation (hot hopping) or complete geometric relaxation occurs prior to hopping and yields fully planar chromophores (weak coupling regime). In principle, if conformational relaxation occurs on a time scale comparable to that of energy transfer, the spectral overlaps and, therefore, also the hopping rates become time-dependent, and memory effects have to be considered when solving the (non-Markovian) master equations for excitation diffusion.[47,48] Here, it turns out that the changes in spectral overlaps incurred through the conformational relaxation processes are very limited so that memory effects can be neglected.

Thus, excitation diffusion occurs through a succession of hopping events in between static chromophores and follows a set of (Markovian) Pauli Master Equations:

$$\frac{dP_i}{dt} = -\left(\sum_{j\neq i} P_i k_{ij} - \sum_{j\neq i} P_j k_{ji} + \frac{P_i}{\tau_i}\right) \qquad (4)$$

where P_i stands for the population on chromophore i, τ_i represents the radiative lifetime of an exciton on site i, and k_{ij} is the (time-independent) hopping rate from one chromophore i to j. The radiative lifetime is obtained from the Einstein's coefficient for spontaneous emission,

$$\tau_i^{-1} = \left(\frac{8\pi^2\nu_i^3}{3\varepsilon_0\hbar c^3}\right)|\mu_i|^2 \qquad (5)$$

where ν_i is the frequency of the lowest electronic transition and μ_i the corresponding transition dipole moment.

III. Conformational Space and Optical Properties

For each torsion potential sketched in Figure 1, a total of ∼100 chains was generated and mapped out into a set of chromophores, and their linear absorption spectra were simulated as the superimposition of the chromophore spectra. Vibronic coupling with two effective modes was included in the simulations, as discussed in the previous section, and the single chromophore spectra were convoluted with Lorentzian functions with a full width at half maximum of 0.1 eV (to account for the conglomerate of acoustic and optical lattice modes). The chains were ∼100 repeating units long, because this is comparable to, yet, even larger than the average physical length reported by Swager and co-workers on a PPE-iptycene copolymer.[23]

Figure 3 portrays the population histograms of the conjugation-length distributions obtained for the different torsion potentials.

From Figure 3, the following can be seen.

- The gas-phase B3LYP calculations yield a narrow distribution in the short conjugation-length region (∼70% of the conjuga-

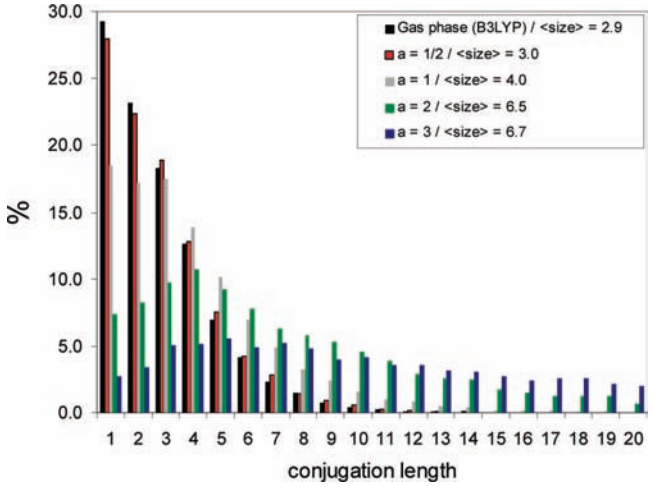

Figure 3. Distribution of conjugation lengths (%) for the different torsion potentials. The average (⟨size⟩) values are given as insert.

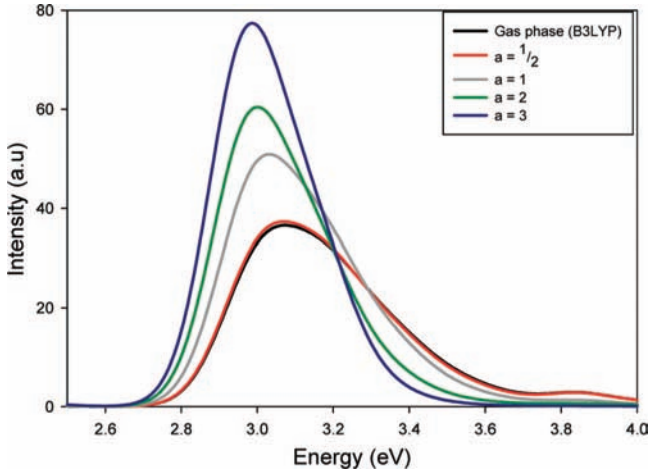

Figure 4. Absorption spectra simulated for several torsion potentials of PPE chains.

tion segments are from 1 to 3 repeating units long). A very similar distribution is obtained, as expected, on the basis of the (1/2) $\sin^2(\phi)$ potential.

- When stiffer potentials are used (increased the value of a in the fitted function $a \sin^2(\phi)$), the overall distribution is continuously shifted to longer segments. At the same time, the number of conjugation breaks evidently decreases.

Thus, the simple trick used to generate the polymer chains gives rise, as anticipated, to chains featuring averaged number of conjugation breaks and delocalization lengths that can be tuned over a broad range.

Figure 4 depicts the absorption spectra corresponding to the conjugation-length distributions reported in Figure 3, averaged over 100 realizations of the polymer chains. Two important features can be noticed when the distribution is displaced toward more planar conformations (stiffer potential). First, the overall absorption spectrum is red-shifted as expected from the increased averaged conjugation length. Second, the absorption bandwidth, which is partly associated with the amount of inhomogeneity (e.g., the presence of static chromophores with different lengths and, hence, excitation energies), decreases concomitantly. These trends are consistent with those observed experimentally by Swager and co-workers when embedding PPE-iptycene chains into a nematic liquid crystal phase instead of a conventional organic solvent.

IV. Excitation Diffusion along Polymer Chains

Table 1 lists the averaged values for the electronic couplings, spectral overlaps, and hopping and radiative decay rates in polymer chains generated on the basis of different torsion potentials. As noted previously, the spectral overlaps calculated at time = 0 (hot transfer) are on average similar to those obtained after complete conformational relaxation on the donor; yet, the latter are slightly smaller than the former because of the torsion-induced Stokes shift that lowers the overlap between donor emission and acceptor absorption.

The following trends can be identified from Table 1.

- Because of the dilution of the wave function and the increased center-to-center distance, the electronic couplings decrease with increasing conjugation lengths.[36,40,41]
- The spectral overlap shows the opposite trend: it increases in going to stiffer potentials as a result of the smaller conformational energetic disorder.
- The hopping rates that scale with the electronic coupling squared follow the V_{da} evolution: they are the smallest in the most constrained torsion potentials.
- Because of the extended π-delocalization (increased oscillator strength), the radiative lifetime decreases with increasing average conjugation length.

Altogether, these results suggest that the electronic excitations should diffuse over smaller distances in the stiffer torsional potentials, because, on average, both the individual hopping rates and the (radiative) lifetimes are smaller. This is apparently at odds with the increased emission from end-caps measured in similar polymer chains dissolved in a LC phase. To get more insight on the excitation transport efficiency, we have performed two set of simulations. In the first case, we model the presence of end-capped emitters by artificially lowering the energy (by 1 eV) of the first and last chromophores along the chains and raising [lowering] (by a factor 2) the excitation hopping rate onto [from] the end caps, so that they act as emissive traps. We have also considered end-capped free polymer chains and extracted the diffusion length from the root-mean-squared displacements.

Figure 5 shows the time-dependent population on the acceptor end-groups in the biased polymer chains for different potentials. The data reported here are obtained by considering the spectral overlaps from fully relaxed subunits. Very similar results (with, as expected, a slightly more efficient energy diffusion to the acceptors) are obtained for the hot-transfer mechanism and will not be discussed further.

All potentials yield a similar picture, with a first raise in the acceptor population arising from energy diffusion along the polymer chains and trapping at the end sites followed by a quasi-monoexponential decay resulting from radiative recombination on the acceptors. In the gas-phase potential, a small fraction (∼15%) of the photoinduced electronic excitations reach the end-caps within their lifetimes; this ratio is increased by almost a factor 3 when going from the flat $a = 1/2$ to the stiff $a = 3$ torsion potential. Thus, the diffusion of the electronic excitations along the polymer chains turns out to be much more efficient in the polymer chains displaying the largest conjugation lengths, despite the fact that, on average, each hopping step takes longer. This apparent contradiction can be rationalized in the following way.

- The percentage of chromophores with small lengths, especially monomer units, gets larger when the torsion potential gets flatter. These units act as kinks for energy diffusion along the chains, because they are characterized by much higher excitation energy than the average; hence, the hopping rate

TABLE 1: Average Energy Hopping Parameters (Electronic Coupling, Spectral Overlap, and Hopping Rates Based on Thermalized or Hot Energy Transfer and Radiative Lifetimes) as a Function of the Torsion Potential Used

potential	$\langle V_{DA}\rangle$ (cm^{-1})	$\langle J_{da}\rangle$ (cm), thermalized	$\langle J_{da}\rangle$ (cm), hot transfer	$\langle k_{da}\rangle$ (ps^{-1}), thermalized	$\langle k_{da}\rangle$ (ps^{-1}), hot transfer	$\langle \tau_R\rangle$ (ps)
gas phase (B3LYP)	119.4	$7.4.10^{-5}$	$8.4.10^{-5}$	1.47	1.6	4140
$a = 1/2$	119.4	$7.4.10^{-5}$	$8.4.10^{-5}$	1.47	1.6	4000
$a = 1$	98.4	$8.1.10^{-5}$	$9.6.10^{-5}$	1.09	1.21	2938
$a = 2$	53.2	1.10^{-4}	$1.3.10^{-4}$	0.52	0.58	2334
$a = 3$	33.1	$1.3.10^{-4}$	$1.77.10^{-4}$	0.34	0.36	1283

to these small subunits is usually very small, so that in these 1D systems, the excitation needs to jump to the next nearest neighbor to keep moving, which results in a decrease of the energy transport efficiency.

- In contrast, going to longer average conjugation lengths narrows the inhomogeneous energetic distribution, as a result of the saturation of the electronic transition energy with size (i.e., the same length distributions centered around either three or six repeating units translate into different energy distributions).

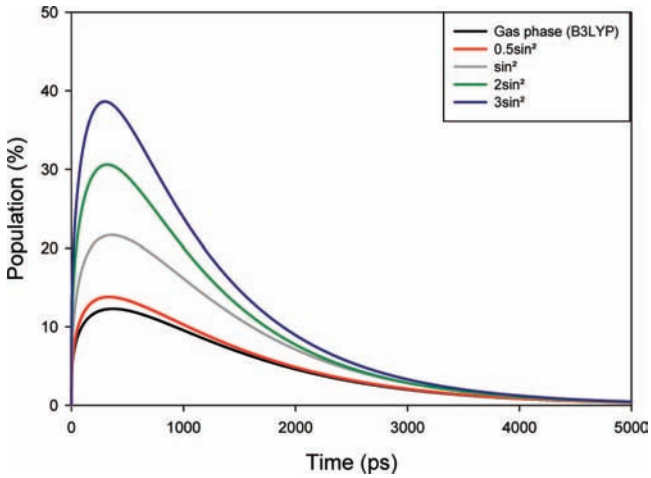

Figure 5. Population (in %) on the final acceptor as a function of time.

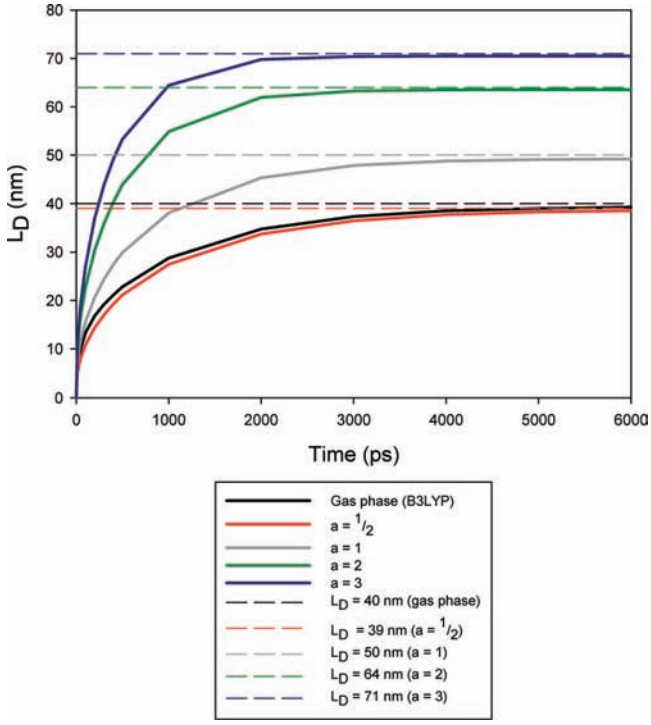

Figure 6. rms displacement (in nm) as a function of time (in ps).

- The increasing conjugation lengths obtained for increasing stiffness leads to a reduced number of chromophores (~40 in gas phase versus ~10 for $a = 3$ in a 100-mer chain). Hence, fewer hopping steps are required to reach the polymer end-caps. In other words, the lower hopping rate is compensated by the longer distance covered in rigid chains (the average hopping distance is ~10nm/step for chains generated with the 3 $\sin^2$ potential but only ~3nm/step in the gas-phase potential).

The determination of diffusion lengths was performed for end-capped free polymer chains by using

$$\frac{\sum_i P_i(t)\langle x_i^2\rangle}{\sum_i P_i(t)} = \langle x^2\rangle(t)$$

$$\sqrt{\langle x^2\rangle(t \to \infty)} = L_D \qquad (6)$$

The results reported in Figure 6 are consistent with the analysis based on biased chains. The rms distance increases with a; that is, the excitations explore longer distances in the torsional potentials with the strongest constraint. This translates into higher diffusion lengths. Note that the L_D values are likely overestimated, because we account in our calculations only for the presence of different conjugation lengths (and hence excitation energies) but not for the different environments felt by these conformers (that would result in a larger inhomogeneity and therefore smaller diffusion lengths). However, this should not affect the conclusion that electronic excitations diffuse further in stiffer polymer chains, in agreement with the experimental data in ref 23.

V. Conclusions

We have investigated excitation diffusion processes along phenylenebutadyine-based polymer chains with different amounts of conformational flexibility. Increasing the stiffness of the torsion potential between repeating units results in chains that are on average more planar and, therefore, yield a red-shifted, narrowed excitation energy distribution. Because of the longer conjugated segments, the electronic coupling mediating excitation hopping is reduced, and so is the overall hopping rate, despite a more favorable spectral overlap. Yet, simulations of transport along free and end-capped polymer chains show that excitation migration is more efficient along chains that display the more constrained potential around the planar conformation, in agreement with the work by Swager and co-workers.[23] We attribute this to a lower degree of inhomogeneity arising from the narrower distribution of conjugation segments and resulting excitation energies together with the larger average hopping distances in the samples with increased conjugation lengths. Within a Förster-type picture, our results imply that longer diffusion lengths can be reached in polymers characterized by smaller Förster radii (that encompass spectral overlap and

electronic coupling factors), provided that this is overcompensated by a smaller degree of static disorder. We are now exploring this interplay further.[49]

Acknowledgment. The work is supported by the Interuniversity Attraction Pole program of the Belgian Federal Government (PAI 6/27), the European Commission via Project MODECOM (NMP-CT-2006-016434), and the Belgian National Fund for Scientific research (FNRS). D.B. is a FNRS research director. B.V.A. acknowledges a grant from FRIA (Fonds pour la Formation à la Recherche dans l'Industrie et dans l'Agriculture).

References and Notes

(1) McQuade, D. T.; Pullen, A. E.; Swager, T. M. *Chem. Rev.* **2000**, *100*, 2537–2574.
(2) Nilsson, K. P. R.; Inganäs, O. *Macromolecules* **2004**, *37*, 9109–9113.
(3) Nilsson, K. P. R.; Olsson, J. D. M.; Konradsson, P.; Inganäs, O. *Macromolecules* **2004**, *37*, 6316–6321.
(4) Björk, P.; Persson, N.-K.; Nilsson, K. P. R.; Åsberg, P.; Inganäs, O. *Biosens. Bioelectron.* **2005**, *20*, 1764–1771.
(5) Nilsson, K. P. R.; Rydberg, J.; Baltzer, L.; Inganäs, O. *Proc. Natl. Acad. Sci. U.S.A.* **2004**, *101*, 11197–11202.
(6) Zhou, Q.; Swager, T. M. *J. Am. Chem. Soc.* **1995**, *117*, 12593–12602.
(7) Thomas, S. W., III; Joly, G. D.; Swager, T. M. *Chem. Rev.* **2007**, *107*, 1339–1386.
(8) McQuade, D. T.; Hegedus, A. H.; Swager, T. M. *J. Am. Chem. Soc.* **2000**, *122*, 12389–12390.
(9) Chen, L.; McBranch, D. W.; Wang, H.-L.; Helgeson, R.; Wudl, F.; Whitten, D. G. *Proc. Natl. Acad. Sci. U.S.A.* **1999**, *96*, 12287–12292.
(10) Wang, D.; Gong, X.; Heeger, P. S.; Rininsland, F.; Bazan, G. C.; Heeger, A. J. *Proc. Natl. Acad. Sci. U.S.A.* **2002**, *99*, 49–53.
(11) Gong, X.; Wang, S.; Moses, D.; Bazan, G. C.; Heeger, A. J. *Adv. Mater.* **2005**, *17*, 2053–2058.
(12) Stork, M.; Gaylord, B. S.; Heeger, A. J.; Bazan, G. C. *Adv. Mater.* **2002**, *14*, 361–366.
(13) Dwight, S. J.; Gaylord, B. S.; Hong, J. W.; Bazan, G. C. *J. Am. Chem. Soc.* **2004**, *126*, 16850–16859.
(14) Dore, K.; Dubus, S.; Ho, H.-A.; Levesque, I.; Brunette, M.; Corbeil, G.; Boissinot, M.; Boivin, G.; Bergeron, M. G.; Boudreau, D.; Leclerc, M. *J. Am. Chem. Soc.* **2004**, *126*, 4240–4244.
(15) Ho, H.-A.; Najari, A.; Leclerc, M. *Acc. Chem. Res.* **2008**, *41*, 168–178.
(16) Hennebicq, E.; Deleener, C.; Bredas, J. L.; Scholes, G. D.; Beljonne, D. *J. Chem. Phys.* **2006**, *125*, 054901.
(17) Russo, V.; Curutchet, C.; Mennucci, B. *J. Phys. Chem. B* **2007**, *111*, 853–863.
(18) Van Averbeke, B.; Beljonne, D.; Hennebicq, E. *Adv. Funct. Mater.* **2008**, *18*, 492–498.
(19) Bässler, H.; Schweitzer, B. *Acc. Chem. Res.* **1999**, *32*, 173–182.
(20) Yu, J.; Hu, D.; Barbara, F. *Science* **2000**, *289*, 1327–1330.
(21) Hennebicq, E.; Pourtois, G.; Scholes, G. D.; Herz, L. M.; Russel, D. M.; Silva, C.; Setayesh, S.; Grimsdale, A. C.; Müllen, K.; Brédas, J.-L.; Beljonne, D. *J. Am. Chem. Soc.* **2005**, *127*, 4744–4762.
(22) Beenken, W. J. D.; Pullerits, T. *J. Phys. Chem. B* **2004**, *108*, 6164–6169.
(23) Nesterov, E. E.; Zhu, Z.; Swager, T. M. *J. Am. Chem. Soc.* **2005**, *127*, 10083–10088.
(24) Scholes, G. D.; Harcourt, R. D.; Ghiggino, K. P. *J. Chem. Phys.* **1995**, *102*, 9574–9581.
(25) Thompson, A. L.; Gaab, K. B.; Xu, J.; Bardeen, C. J.; Martinez, T. J. *J. Phys. Chem. A* **2004**, *108*, 671–682.
(26) Dahlbom, M.; Beenken, W.; Sundström, V.; Pullerits, T. *Chem. Phys. Lett.* **2002**, *364*, 556–561.
(27) Westenhoff, S.; Beenken, W. J. D.; Friend, R. H.; Greenham, N. C.; Yartsev, A.; Sundström, V. *Phys. Rev. Lett.* **2006**, *97*, 166804.
(28) Drobizhev, M.; Rebane, A.; Sigel, C.; Elandaloussi, E. H.; Spangler, C. W. *Chem. Phys. Lett.* **2000**, *325*, 375–382.
(29) Hohenberg, P.; Kohn, W. *Phys. Rev.* **1964**, *136*, B864−B871.
(30) Kohn, W.; Sham, L. J. *Phys. Rev.* **1965**, *140*, A1133−A1138.
(31) Becke, A. D. *J. Chem. Phys.* **1993**, *98*, 5648.
(32) Lee, C.; Yang, W.; Parr, R. G. *Phys. Rev. B* **1988**, *37*, 785.
(33) Petersson, G. A.; Al-Laham, M. A. *J. Chem. Phys.* **1991**, *94*, 6081.
(34) Li, N.; Jia, K.; Wang, S.; Xia, A. *J. Phys. Chem. A* **2007**, *111*, 9393–9398.
(35) Magyar, R. J.; Tretiak, S.; Gao, Y.; Wang, H. L.; Shreve, A. P. *Chem. Phys. Lett.* **2005**, *401*, 149.
(36) Beljonne, D.; Cornil, J.; Silbey, R.; Millié, P.; Brédas, J. L. *J. Chem. Phys.* **2000**, *112*, 4749–4758.
(37) Wong, K. F.; Bagchi, B.; Rossky, P. J. *J. Phys. Chem. A* **2004**, *108*, 5752–5763.
(38) Barford, W. *J. Chem. Phys.* **2007**, *126*, 134905.
(39) Scholes, G. D.; Fleming, G. R. *J. Phys. Chem. B* **2000**, *104*, 1854–1868.
(40) Hennebicq, E.; Pourtois, G.; Scholes, G. D.; Herz, L. M.; Russell, D. M.; Silva, C.; Setayesh, S.; Grimsdale, A. C.; Mullen, K.; Bredas, J.-L.; Beljonne, D. *J. Am. Chem. Soc.* **2005**, *127*, 4744–4762.
(41) Westenhoff, S.; Abrusci, A.; Feast, W. J.; Henze, O.; Kilbinger, A. F. M.; Schenning, A. P. H. J.; Silva, C. *Adv. Mater.* **2006**, *18*, 1281–1285.
(42) Mataga, N.; Nishimoto, K. *Z. Phys. Chem.* **1957**, *13*, 140.
(43) Ridley, J.; Zerner, M. C. *Theor. Chim. Acta.* **1973**, *32*, 111.
(44) Karaburnaliev, S.; Bittner, E.; Baumgarten, M. *J. Chem. Phys.* **2001**, *114*, 5863.
(45) Dewar, M. J. S.; Zoebisch, E. G.; Healy, E. F.; Stewart, J. J. P. *J. Am. Chem. Soc.* **1985**, *107*, 3702.
(46) The active space in the CI calculations includes the most frontier $4n + 4$ occupied (unoccupied) molecular orbitals, where n is the number of repeating units.
(47) Kimura, A.; Kakitani, T. *J. Phys. Chem. A.* **2007**, *111*, 12042–12048.
(48) Kimura, A.; Kakitani, T.; Yamato, T. *J. Phys. Chem. B.* **2000**, *104*, 9276–9287.
(49) Athanasopoulos, in preparation.

JP810815D